Journal of Sound and Vibration (1997) **208**(3), 491–496

LETTERS TO THE EDITOR

ON THE TURBULENT JET NOISE NEAR AN IMPEDANCE SURFACE

S. Taherzadeh and K. M. Li
Engineering Mechanics Discipline, Faculty of Technology, The Open University, Milton Keynes MK7 6AA

(*Received* 6 *June* 1997, *and in final form* 25 *July* 1997)

1. Introduction

In a recent study, Smith and Carpenter [1] applied Lighthill's acoustic analogy to model the sound radiated by a volume of jet-type shear layer turbulence and calculated the basic directivity patterns of ensemble-averaged noise generated by randomly orientated quadrupoles near a rigid surface. The patterns for the two types of quadrupole, namely longitudinal and lateral quadrupoles, have been shown to be very different from one another and also from the free field case. Their analysis, however, is confined to the case of an acoustically rigid surface. Asymptotic expressions for the sound field of an arbitrarily orientated dipole, and quadrupole, in the vicinity of an impedance boundary have been developed recently [2–4]. The sound field due to an arbitrarily orientated quadrupole is expressed in a convenient form for calculating the ensemble-averaged sound field efficiently. In this communication the theory is used to predict the effect of an impedance plane on the ensemble averaged directivity patterns of quadrupole sources. The analysis is restricted to the case of low subsonic jet noise.

2. Asymptotic expression for a quadrupole source

The sound pressure of an arbitrarily orientated quadrupole above a surface with an acoustic surface admittance of β can be expressed in an asymptotic form as [3]

$$p \approx \frac{-S_2 k^2}{4\pi}\left\{(\mathbf{l}\cdot\hat{\mathbf{R}}_1)(\mathbf{m}\cdot\hat{\mathbf{R}}_1)\frac{\mathrm{e}^{ikR_1}}{R_1} + [(\mathbf{l}\cdot\hat{\mathbf{R}}_2)(\mathbf{m}\cdot\hat{\mathbf{R}}_2)R_p\right.$$

$$\left.+(\mathbf{l}\cdot\hat{\mathbf{R}}_s)(\mathbf{m}\cdot\hat{\mathbf{R}}_s)(1-R_p)F(w)]\frac{\mathrm{e}^{ikR_2}}{R_2}\right\} + \frac{S_2}{4\pi}[(\mathbf{l}\cdot\mathbf{m}) - 3(\mathbf{l}\cdot\hat{\mathbf{R}}_1)(\mathbf{m}\cdot\hat{\mathbf{R}}_1)]\frac{\mathrm{i}kR_1 - 1}{R_1^2}\frac{\mathrm{e}^{ikR_1}}{R_1}$$

$$+\frac{S_2}{4\pi}[(\mathbf{l}\cdot\mathbf{m}) - 3(\mathbf{l}\cdot\hat{\mathbf{R}}_2)(\mathbf{m}\cdot\hat{\mathbf{R}}_2)]\frac{\mathrm{i}kR_2 - 1}{R_2^2}\frac{\mathrm{e}^{ikR_2}}{R_2}, \tag{1a}$$

where R_p, $F(w)$ and w are, respectively, the plane wave reflection coefficient, the boundary loss factor and the numerical distance given by

$$R_p = (\cos\theta_s - \beta)/(\cos\theta_s + \beta), \tag{1b}$$

$$F(w) = 1 + \mathrm{i}\pi^{1/2} w\, \mathrm{e}^{-w^2}\operatorname{erfc}(-\mathrm{i}w), \qquad w = +(\tfrac{1}{2}\mathrm{i}kR_2)^{1/2}(\beta + \cos\theta_s) \tag{1c, d}$$

with θ_s being the angle of incidence. (For detailed discussions on sound propagation from a point source above an impedance plane see references [5, 6].)

The quantity $\hat{\mathbf{R}}_s \equiv (\sin\mu_p\cos\psi_s, \sin\mu_p\sin\psi_s, \cos\mu_p)$ may be regarded as the unit vector that characterizes the direction of the surface wave pole. The angle ψ_s is the azimuthal angle

0022–460X/97/480491 + 06 $25.00/0/sv971215 © 1997 Academic Press Limited

of the line joining the image source to the receiver and the complex angle μ_p is determined by $\cos \mu_p + \beta = 0$. The quantities R_1 and R_2 are the distances from the source and the image source to the receiver respectively, and $\hat{\mathbf{R}}_1$ and $\hat{\mathbf{R}}_2$ are the corresponding unit vectors pointing radially outward from the quadrupole and image centres to the receiver points; see Figure 1(a). The direction cosines **m** and **l** are vectors denoting the direction of the quadrupole axis and its constituent dipoles respectively; see Figure 1(b). They are given by

$$\mathbf{l} = (\sin \gamma_l \cos \psi_l, \sin \gamma_l \sin \psi_l, \cos \gamma_l) \tag{2}$$

and

$$\mathbf{m} = (\sin \gamma_m \cos \psi_m, \sin \gamma_m \sin \psi_m, \cos \gamma_m), \tag{3}$$

where γ_i and ψ_i are the polar and azimuthal angles respectively. For a longitudinal quadrupole the two vectors are parallel and for a lateral one they are perpendicular. In the following calculations, a two-parameter impedance model [7] is used, where the normalized specific admittance, β of the ground is given by

$$1/\beta = 0{\cdot}436\sqrt{\sigma_e/f} + \mathrm{i}[0{\cdot}436\sqrt{\sigma_e/f} + 19{\cdot}48(\alpha_e/f)], \tag{4}$$

where f is frequency, and σ_e and α_e are the effective flow resistivity and effective rate of change of porosity with depth, respectively. This model applies to a rigid porous ground in which the porosity decreases with depth in an exponential form. It has been used with tolerable success to fit excess attenuation data taken indoors and outdoors. The parameter values for σ_e and α_e are assumed to be 100 kPa s m^{-2} and 20 m^{-1} in all calculations. These values are typical of a grass-covered ground.

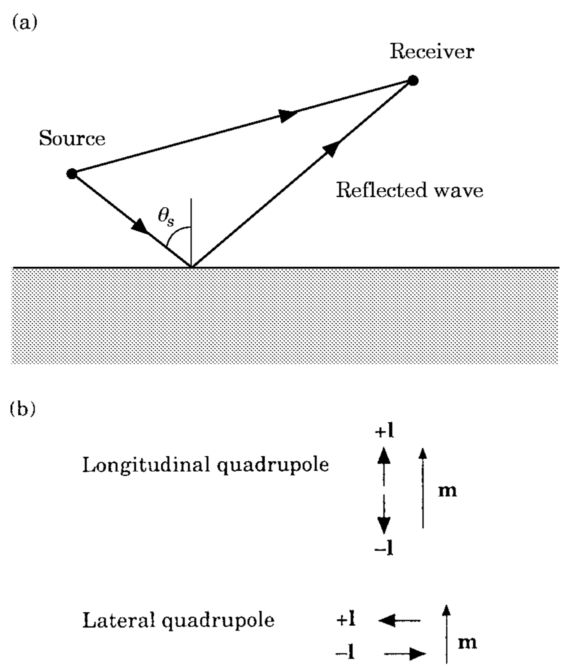

Figure 1. (a) The source–receiver geometry, with θ_s being the incident angle; (b) the two basic types of quadrupole, a longitudinal quadrupole and a lateral quadrupole. The directions of the arrows indicate the orientation of the dipole axis (**l**) and the quadrupole axis (**m**).

3. ENSEMBLE-AVERAGED SOUND FIELD DUE TO QUADRUPOLE SOURCES

The asymptotic solution for an arbitrarily orientated quadrupole may be applied to predict jet noise above an impedance ground. Here, the primary concern is with the fundamental interference effects due to an impedance ground. The following calculations are for the sound fields due to longitudinal and lateral quadrupoles.

First to be shown are the polar plots (in the plane of $y = 0$) of the far field sound pressures due to a longitudinal quadrupole and a lateral quadrupole above an impedance ground (solid line) and a rigid boundary (dotted line). The source is 0·11 m above the ground and the frequency is 1000 Hz. In Figures 2(a) and 2(b) it is shown that the sound fields due to a longitudinal and a lateral quadrupole above a finite impedance ground are significantly different from those above a rigid plane.

The ensemble-averaged intensity $I_l(\theta)$ of a randomly orientated longitudinal quadrupole can be calculated by [1]

$$I_l(\bar{\theta}) = \frac{1}{2\pi^2} \int_{\psi_m = 0}^{2\pi} \int_{\gamma_m = 0}^{\pi} \frac{|p|^2}{\rho c} \, \mathrm{d}\gamma_m \, \mathrm{d}\psi_m. \tag{5}$$

In the case of a rigid surface ($\beta = 0$) the integral (5) can be evaluated explicitly in the far field to give

$$I_l(\bar{\theta}) = K_l \{[\cos^4\bar{\theta} - \tfrac{1}{4}\sin^4\bar{\theta} + 1 - \tfrac{8}{3}\sin^2\bar{\theta}\cos^2\bar{\theta}]\cos^2(kz_s\cos\bar{\theta}) + \tfrac{4}{3}\sin^2\bar{\theta}\cos^2\bar{\theta}\}, \tag{6}$$

with k being the wavenumber and z_s the source height. The constant parameter K_l is a function of ρ, R, c and k. The exact value of K_l is less important since one is interested in the directivity patterns for $I_l(\bar{\theta})$ (the curly bracket of equation (6)). The far field intensity specified in equation (6) furnishes a small correction, $\cos^4\bar{\theta} - \frac{1}{4}\sin^4\bar{\theta}$, to the result obtained

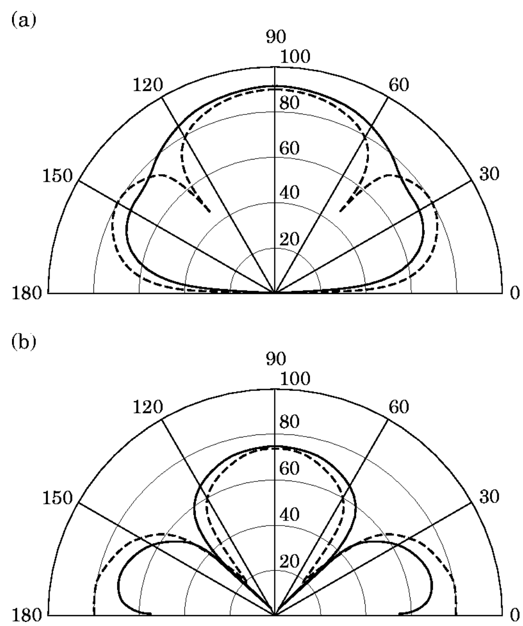

Figure 2. The directivity pattern, the x–y plane, of the far field sound pressure due to a quadrupole above rigid surface (dashed lines) and an impedance surface (solid lines). The frequency is 1000 Hz and the source is 0·11 m above the surface. (a) A longitudinal quadruple with **l** and **m** perpendicular to the surface; (b) a lateral quadrupole with **l** perpendicular and **m** parallel to the surface.

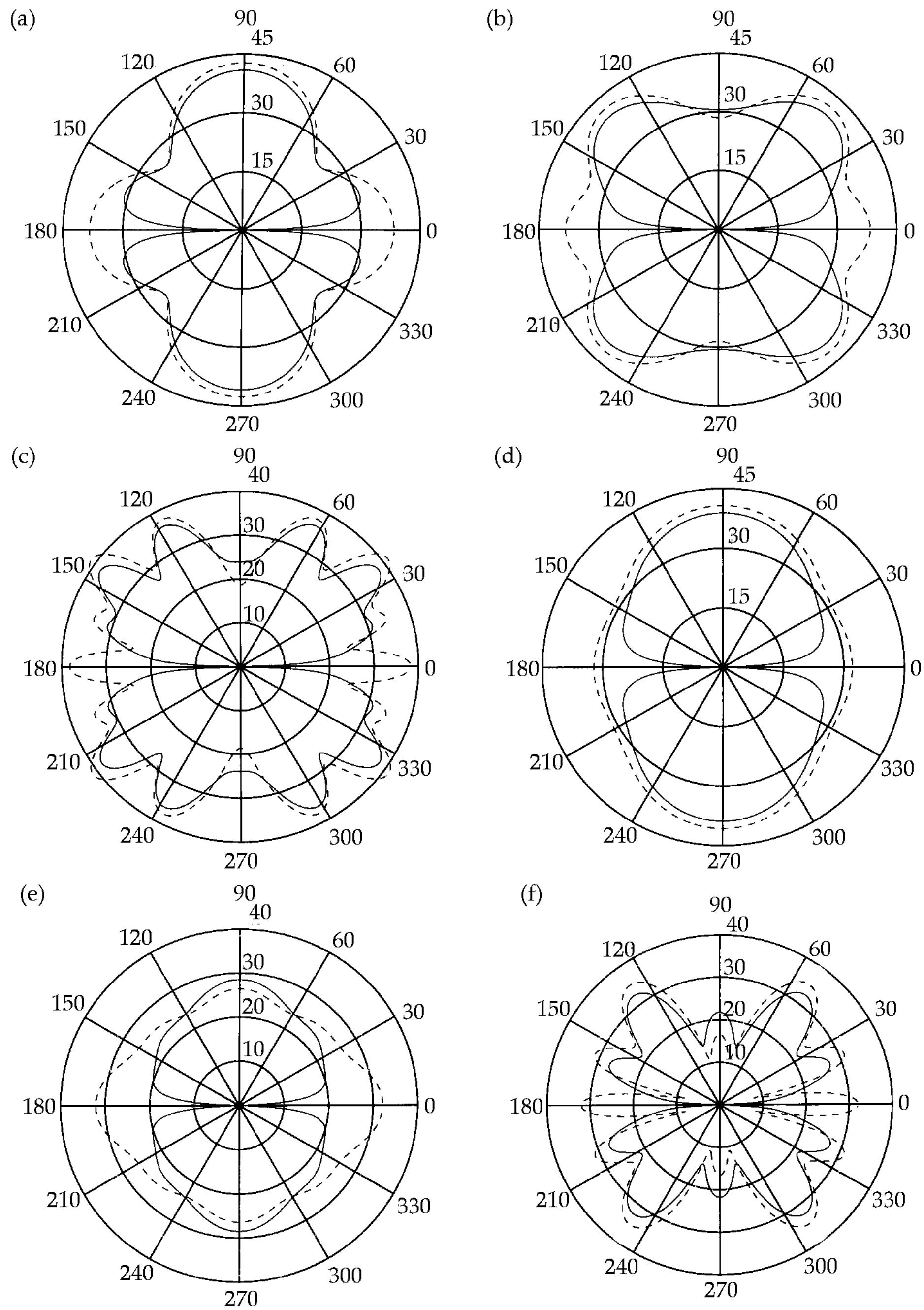

Figure 3. The polar plot in the x–z plane of an ensemble-averaged far field intensity of a randomly orientated quadrupole above a rigid boundary (dashed line) and an impedance boundary (solid line). The frequency in all cases is 1000 Hz. (a) A lateral quadrupole with $kz_s = 0$; (b) lateral quadrupole with $kz_s = 2$; (c) a lateral quadrupole with $kz_s = 8$; (d) a longitudinal quadrupole with $kz_s = 0$; (e) a longitudinal quadrupole with $kz_s = 2$; (f) a longitudinal quadrupole with $kz_s = 8$.

by Smith and Carpenter [1]. The formula given in equation (6) also agrees with the results obtained by integrating equation (5) numerically.

It is slightly more complicated to calculate the ensemble average of the far field intensity for a randomly oriented lateral quadrupole because the polar and azimuthal angles are determined according to $\mathbf{l} \cdot \mathbf{m} = 0$, or in other words

$$\sin\gamma_l \sin\gamma_m \cos(\psi_l - \psi_m) + \cos\gamma_l \cos\gamma_m = 0. \tag{7}$$

Consequently, three angles are needed to specify fully the orientation of a lateral quadrupole. In the numerical analysis, γ_m, ψ_m and ψ_l are chosen and the polar angle γ_l can be determined explicitly through the use of equation (7). The ensemble average of the far field intensity for a lateral quadrupole can be determined according to

$$I_2(\bar{\theta}) = \frac{1}{4\pi^3} \int_{\psi_l=0}^{2\pi} \int_{\psi_m=0}^{2\pi} \int_{\gamma_m=0}^{\pi} \frac{|p|^2}{\rho c}\, \mathrm{d}\gamma_m\, \mathrm{d}\psi_m\, \mathrm{d}\psi_l. \tag{8}$$

Due to the presence of the ground wave term, it is generally not possible to express the far field intensities in closed form analytic expressions for the case of an impedance ground. Nevertheless, it is relatively simple to evaluate the double integral of equation (5) and the triple integral of equation (8) numerically by standard quadrature routines. The details of this numerical implementation will not be described here.

Using equations (5) and (8), one can compute the ensemble intensity due to longitudinal and lateral quadrupoles. The comparisons are made for the far field intensities above an impedance ground (solid line) and a rigid plane (dashed line) in Figures 3(a)–(f) for different values of kz_s. The far field intensities above an impedance ground are different from those above a rigid plane for both types of quadrupoles. Powell [8] showed that the amplitude of the far field intensity is minimum at 45° to a plane surface for lateral quadrupoles close to a rigid plane. Figure 3(b), for example, suggests that this will not be the case for an elevated source and for the source above an impedance ground. The exact position of the minimum intensity depends on the source height, frequency and the impedance of the ground. The most significant influence of the impedance of ground surface on the directivity is the near cancellation of the intensity field at the grazing angle. This is the same for both longitudinal and lateral quadrupole averages. The other important effect on the directivity pattern of the impedance surface is that the pattern is explicitly dependent on the frequency and the source height rather than the product kz_s. This is caused by the frequency dependence of the reflected wave term.

ACKNOWLEDGMENT

This work was supported by the Engineering and Physical Science Research Council through grant ref. no. GR/L 15236.

REFERENCES

1. C. Smith and P. W. Carpenter 1995 *Journal of Sound and Vibration* **185**, 397–413. The effect of solid surfaces on turbulent jet noise.
2. K. M. Li, S. Taherzadeh and K. Attenborough 1997 *Journal of the Acoustical Society of America* **101**(6), 3343–3352. Sound propagation from a dipole source near an impedance plane.
3. K. M. Li and S. Taherzadeh 1997 *Journal of the Acoustical Society of America*. The sound field of an arbirarily-orientated quadrupole near ground surfaces.
4. S. Taherzadeh 1996 *Ph.D. Thesis*, *The Open University*. Sound propagation in inhomogeneous media.

5. C. F. CHIEN and W. W. SOROKA 1975 *Journal of Sound and Vibration* **81**, 413–424. Sound propagation along an impedance boundary.
6. M. R. STINSON 1995 *Journal of the Acoustical Society of America* **98**, 1810–1813. A note on the use of an approximate formula to predict sound fields above an impedance plane due to a point source.
7. K. ATTENBOROUGH 1992 *Journal of the Acoustical Society of America* **92**, 418–427. Ground parameter information for propagation modeling.
8. A. POWELL 1994 *Journal of the Acoustical Society of America* **96**, 590–593. Nature of the sound sources in low-speed jet impingement—further investigation.